Int. J. Nano Dimens., 9 (3): 246-259, Summer 2018

ORIGINAL ARTICLE

Adsorption study of Zinc ion onto halloysite nanotubes using taguchi's design of experimental methodology

*Gholamreza Kiani [1, *]; Mehdi Soltanzadeh [1]; Iraj Ahadzadeh [2]*

[1]*School of Engineering-Emerging Technologies, University of Tabriz, Tabriz, Iran*
[2]*Department of Physical Chemistry, Faculty of Chemistry, University of Tabriz, Tabriz, Iran*

Received 13 January 2018; revised 06 March 2018; accepted 27 April 2018; available online 28 April 2018

Abstract

In this paper, Taguchi method was applied to determine the optimum conditions for Zn (II) removal from aqueous solution by halloysite nanotubes (HNTs). An orthogonal array experimental design (L_{16} (4^5) which is of five control factors including pH, t (contact time), m (adsorbent mass), T (temperature) and C_0 (initial concentration of Zn (II)) having four levels was employed. Adsorption capacity (mg/g) and removal percent (%) were investigated as the quality characteristics to be optimized. In order to determine the optimum levels of the control factors precisely, range analysis and analysis of variance were performed. For removal percent, the optimum condition was found to be pH=6, T=35°C, w=0.4 g, and C_0=50 mg/L. Under these optimum conditions, adsorption capacity and removal percent can reach to 132.16 mg/g and 99.76%, respectively.

Keywords: *Adsorption; Halloysite Nanotubes; Heavy metal ions; Optimization; Taguchi method.*

How to cite this article

Kiani G, Soltanzadeh M, Ahadzadeh I. Adsorption study of Zinc ion onto Halloysite nanotubes using taguchi's design of experimental methodology. Int. J. Nano Dimens. 2018; 9 (3): 246-259.

INTRODUCTION

Environmental pollution caused by toxic heavy metals is one of the most serious problems in many densely populated cities worldwide. The industrial and domestic wastes responsible for various damages to the environment adversely affect the health of the human population. Several catastrophic events resulting from heavy metal contamination in the aquatic environment increased the awareness of the heavy metal toxicity [1]. Most of these processes are not widely accepted due to their high costs, low efficiency, disposal of sludge, inapplicability to a wide range of pollutants [2]. The adsorption process is arguably one of the more popular methods for the removal of heavy-metal ions because of its simplicity, convenience, and high removal efficiency [3-9].

Halloysite is a clay mineral with a nano-scaled tubular structure that acts as an effective adsorbent. Halloysite has attracted much attention due to its excellent properties such as availability, biocompatibility, and ecofriendly feature [10]. Recently, halloysite and its composite structures have been used for adsorption of various molecules and contaminants such as dyes, benzene, alcohols, halides, carboxylic acids, drugs, and heavy metals [10-15].

Zinc is a trace element that is essential for human health. When people absorb too little zinc they can experience a loss of appetite, decreased sense of taste and smell, slow wound healing and skin sores. Zinc-shortages can even cause birth defects. Although humans can handle proportionally large concentrations of zinc, too much zinc can still cause eminent health problems, such as stomach cramps, skin irritations, vomiting, nausea and anemia. Very high levels of zinc can damage the pancreas and disturb the protein metabolism, and cause arteriosclerosis. Extensive exposure to zinc chloride can cause respiratory disorders [16, 17]. So the removal of zinc from environment is essential.

Design of experiments (DOE) develops a scheme of experimental different conditions. The Taguchi method was established by Genichi Taguchi [18]. Taguchi optimization technique is a

* Corresponding Author Email: g.kiani@tabrizu.ac.ir

unique and powerful optimization discipline that allows optimization with minimum number of experiments [19]. The Taguchi crossed array layout consists of an inner array and an outer array. The inner array is made up of the orthogonal array (OA) selected from all possible combinations of the controllable factors. Using the orthogonal array specially designed for the Taguchi method, the optimum experimental conditions can be easily determined. Taguchi method is capable of establishing an optimal design configuration, even when significant interaction exists between and among the control variables. Also the Taguchi's design can further be simplified by expanding the application of the traditional experimental designs to the use of orthogonal array. The Taguchi method has applications in different fields such as medicine, water treatment, mechanical and electrical engineering [20-23]. Taguchi method in comparison with the other experimental design methods works with lower number of experiments to determine the optimized condition that cause to faster evaluation and low cost. In this method the selections are fully randomized and more accurate predictions are achievable. On the other hand, the signal to noise factor is only meaningful in Taguchi experimental method. The disadvantage of this method is to need for a "burn storm" to happen before experimental design. It means that the initial evaluations are needed before design of experiment to partly predict the optimized condition [24]. In this study, the Taguchi orthogonal experimental design was applied to optimize the operational conditions for the adsorption of zinc heavy metal ions onto halloysite (HNT) from aqueous solution. In fact a powerful experimental design method was used to make easy, fast, and accurate experimental investigation for optimization of broad range of affecting parameters in the zinc ion removal from aqueous solution. In continuing the affecting parameters on the adsorption of the Zn ions by an orthogonal array design, five factors-four levels 4^5 matrices, were optimized. Furthermore, the analysis of variances was employed to investigate the optimum test parameters for better removal percent or removal rate.

EXPERIMENTAL

Halloysite (premium grade) was obtained from New Zealand, China Clays Ltd (New Zealand). Halloysite was first sieved (125 µm mesh) to remove granules to obtain 42% fine powder (HNTs).

This study considers five controllable factors, and each factor has four levels (Table 1). Therefore, an L_{16} (4^5) orthogonal array (OA) is chosen, and the experimental conditions (Table 2) can be obtained by combining Table 1 and the L_{16} (4^5) orthogonal array. Stock solutions of 1000 mg/L Zn (II) were prepared from Zn $(NO_3)_2$ as the Zn source in deionized water. A series of Zn aqueous solutions with the contact time of 10-100 min, initial concentration of 50-140 ppm, dose of 0.1-0.4 g/100mL, a temperature of 20-65°C, and pH of 3-6 were prepared. The data were achieved by two or three times measurements.

Table 1 shows five factors and four levels used in the experiment. If four levels were assigned to each of these factors and a factorial experimental design was employed using each of these values, the number of permutations would be 625. The fractional factorial design reduced the number of experiments to sixteen. The pH value (A), temperature (B), contact time (C), adsorbent mass (D) and initial zinc ion concentration (E) were

Table 1: Controllable factors and their levels.

Process parameter	Designation	Level 1	Level 2	Level 3	Level 4
PH	A	3	4	5	6
Temperature (°C)	B	20	35	50	65
Contact time (min)	C	10	40	70	100
Sorbent mass (g)	D	0.1	0.2	0.3	0.4
Initial Zn (II) conc. (mg/L)	E	50	80	110	140

assigned to the 1st, 2nd, 3rd, 4th and the 5th column of L_{16} array respectively. The orthogonal array of L_{16} type was used and is represented in Table 2. This design requires sixteen experiments with five parameters at each of these four levels.

Statistical analysis

The parameter design phase of the Taguchi method generally includes the following steps: (1) identify the objective of the experiment; (2) identify the quality characteristic (performance measure) and its measurement systems; (3) identify the factors that may influence the quality characteristic, their levels and possible interactions; (4) select the appropriate OA and assign the factors at their levels to the OA; (5) conduct the test described by the trials in the OA; (6) analyze the experimental data using the standard analysis, factor effects and the ANOVA (analysis of variance) to see which factors are statistically significant, and find the optimum levels of factors; (7) verify the optimal design parameters through confirmation experiment.

Data analysis method

The collected data were analyzed by Qualitek-4 statistical software for the evaluation of the effect of each factor on the adsorption process. For the range analysis and the analysis of variance (ANOVA) of the data in the Taguchi method, experimental design, Qualitek-4 statistical software was also used.

Calculation of the adsorption capacity and removal percent

The adsorption capacity and the removal percent of removing Zn (II) from aqueous solutions by HNTs were calculated by the following equations (1, 2):

$$q_{eq} = V(C_0 - C_t)/W \quad (1)$$

$$n = (C_0\text{-}C_e)/C_0 \times 100\% \quad (2)$$

where q_{eq} is the adsorption capacity (mg $_{metal}$/g $_{adsorbent}$); n is the removal percent (%); C_0 is the initial Zn (II) concentration (mg/L), C_e is the equilibrium Zn (II) concentration (mg/L), W is the adsorbent mass (g) and V is the volume of metal solution put in contact with the adsorbent [25].

Characterization

Transmission electron micrographs (TEM) of halloysite nanotubes were obtained by use of a JEOL JEM-2100 (Japan) microscope. X-ray diffraction (XRD) pattern was achieved by D500 Siemens, X-Ray diffractometer. The Zn ion concentrations were measured by atomic absorption spectroscopy (AA 55B, Varian SLM, USA) at room temperature.

Table 2: Experimental design (according to L_{16} (4^5)) and the responses.

Experiment no.	Operating factors and their levels				
	A	B	C	D	E
1	1	1	1	1	1
2	1	2	2	2	2
3	1	3	3	3	3
4	1	4	4	4	4
5	2	1	2	3	4
6	2	2	1	4	3
7	2	3	4	1	2
8	2	4	3	2	1
9	3	1	3	4	2
10	3	2	4	3	1
11	3	3	1	2	4
12	3	4	2	1	3
13	4	1	4	2	3
14	4	2	3	1	4
15	4	3	2	4	1
16	4	4	1	3	2

The levels are shown in Table 1, *A* pH, *B* temperature *C* contact time, *D* sorbent mass, *E* initial Zn (II) conc.

RESULTS AND DISCUSSION

Characterization of Halloysite nanotubes

TEM micrographs were used to investigate the morphology of halloysite nanotubes. Fig. 1 shows the TEM images of the halloysite nanotubes in two magnifications. The hollow tubular structure is clearly visible from TEM images. The halloysite is predominately tube with a length of 0.5-1 µm and an inner diameter of 20-30 nm.

X-ray diffraction pattern of halloysite nanotubes was also achieved to evaluate the crystal structure of that. Fig. 2 shows the XRD pattern of halloysite nanotubes that presents the characteristic peaks of HNT [26].

Effect of pH on Zn (II) uptake

The pH should be an important factor affecting the uptake of heavy metal ions from aqueous solutions by the adsorbent. The pH values selected were prior to the precipitation limit of the metal ions. As can be seen in Fig. 3, removal percent increased with increasing solution pH and a maximum value was reached at around pH 6.00. Increasing pH from 3 to 6 resulted in highest removal percent. This may be attributed to the increased solubility of Zn (II) at high pH values. Taking these theories and results into account, pH 6 was chosen as the best level for further experiments. The removal of Zn (II) from water by HNTs was found to be dependent on the solution pH value. The increase in the metal removal as the pH increases is on the basis of a decrease in competition between proton and metal species for the surface sites, and by the decrease in positive surface charge, which results in a lower columbic repulsion of the sorbing metal ions.

Science the point of zero charge of the halloysite nanotubes is 2.9, the adsorption capacity of HNT in the solution with pH>2.9 is very higher than that of pH < 2.9 [27]. Therefore the experiments were done in the pH=3 or higher. According to the speciation diagram of Zn ions, Zn^{2+} ions are dominant up to pH~8 and in the higher pHs $Zn(OH)_2$, $Zn(OH)_3^-$ and $Zn(OH)_4^{2-}$ are dominant respectively [28]. So the Zn^{2+} is conquering ion in the pH range of present work (pH=3-6).

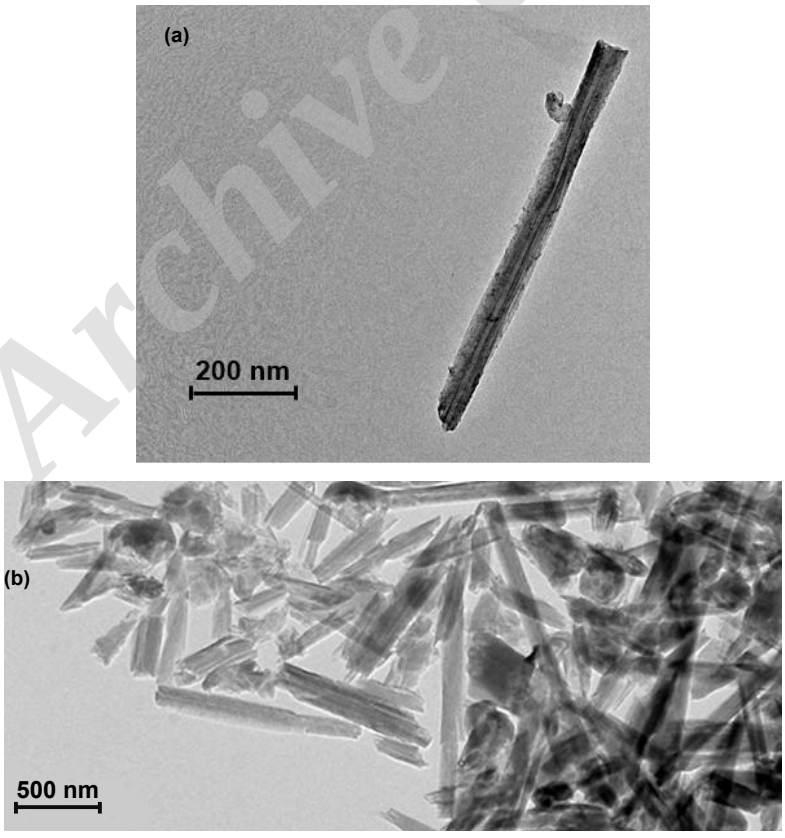

Fig. 1: TEM images of HNTs in two magnifications.

At low pH values, the removal mechanism of Zn^{2+} is complexation and/or cation exchange with H^+ ions present on the outer surface of halloysite, whereas at higher pH values complexation with inner surface could happen [29]. A schematic presentation for adsorption of Zn ion onto halloysite nanotubes is shown in Fig. 4.

Effect of temperature on Zn (II) uptake

Fig. 5 shows the recovery obtained at different temperatures from 20°C to 65°C. The results obtained indicate that 35°C temperature is sufficient to remove Zn ions**.**

It seems that the mobility of molecules increases with increasing temperature up to 35°C that facilitate the formation of adsorbed layers. Further increasing of temperature could decrease the adsorption capacity due to desorption [3].

Effect of contact time on Zn (II) uptake

As can be seen in Fig. 6, during the first 10 min time interval, there was a faster rate of adsorption, and the adsorption amount can reach about 89.2 % of the maximum adsorption capacity.

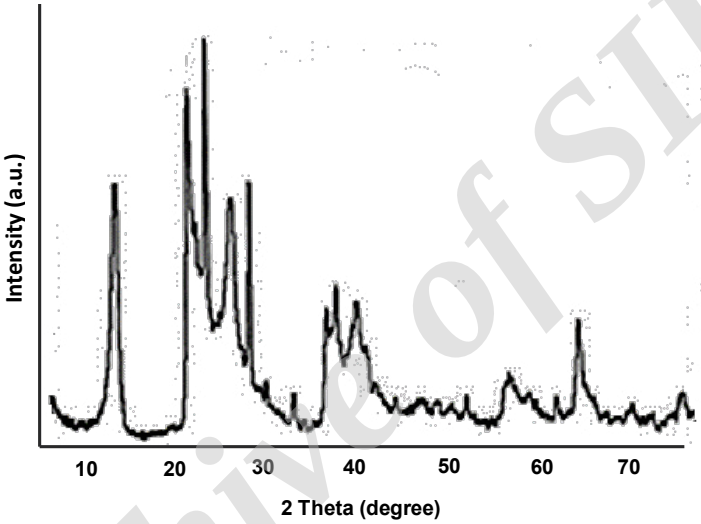

Fig. 2: XRD patterns of HNTs.

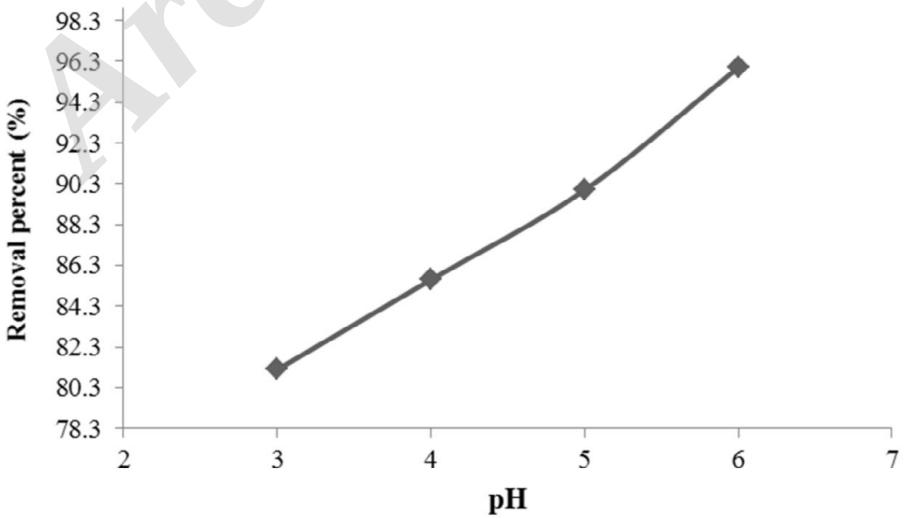

Fig. 3: The effect of pH on the removal percent of Zn (II). Circles on figures indicate optimum pH for adsorption process.

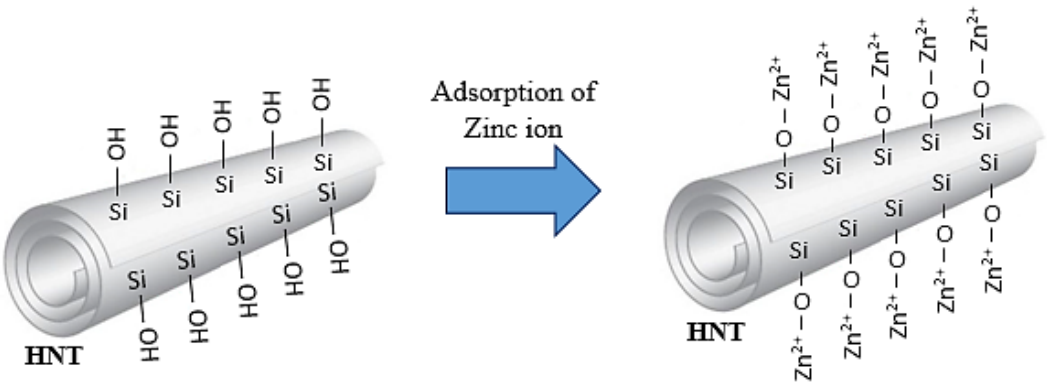

Fig. 4: Schematic presentation for adsorption of Zinc ion onto halloysite nanotubes.

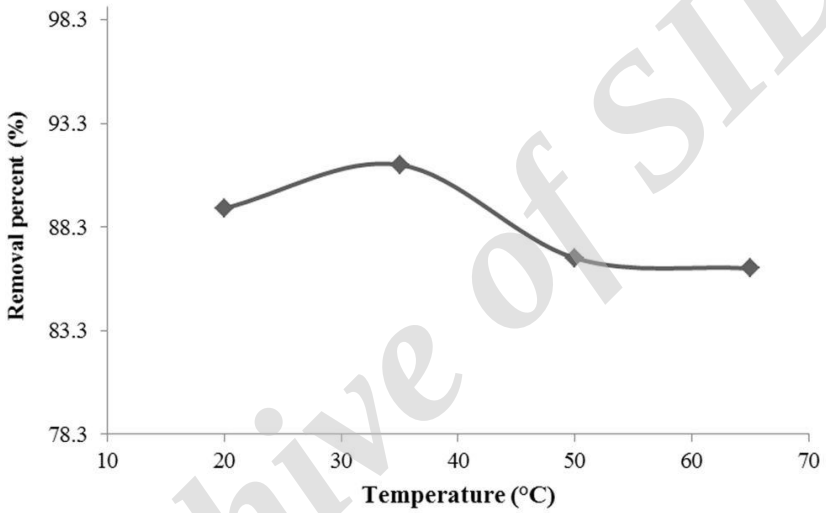

Fig. 5: The effect of temperature on the removal percent of Zn (II). Circles on figures indicate optimum temperature for adsorption process.

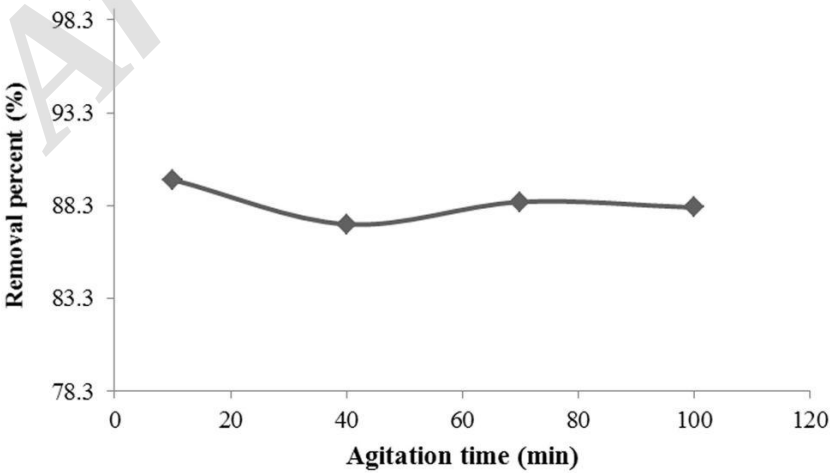

Fig. 6: The effect of agitation time on the removal percent of Zn (II). Circles on figures indicate optimum time for adsorption process.

This fast metal uptake by the adsorbents may be attributed to the abundant availability of active sites on the adsorbent and its highly porous and mesh-like structure, which provides ready access and large surface area for the adsorption of metals on the binding sites [30]. It is seen that the time required for equilibrium is 10 min. In the other words, the optimum time is 10min. This is obvious from the fact that a large number of vacant surface sites are available for the adsorption during the initial stage and with the passage of time, the remaining vacant surface sites are difficult to be occupied due to repulsive forces between the solute molecules on the solid phase and in the bulk liquid phase. Heavy metal adsorption slightly decreases after 10 min. It may be related to desorption process at upper time [31].

Effect of adsorbent mass on Zn (II) uptake

The maximum metal ion removal percent was observed at 0.4 g adsorbent mass per 100 ml zinc ion solution. As it is shown in Fig. 7, an increase in the adsorbent mass strongly affected the removal of Zn (II) ions from aqueous solutions. This indicates that as the adsorbent mass increased, the unoccupied adsorption sites became more surplus with every increase of the biomass. Therefore, 0.4 g was chosen as the best level for further experiments.

Effect of initial Zn (II) concentration on Zn (II) uptake

The heavy metal uptake mechanism is particularly dependent on the initial concentration of the Zn (II). Removal percent of the adsorbent decreased with increasing metal ion concentration in the medium. The maximum removal percent achieved is about 92% under initial concentration of 50 mg/L (Fig. 8). Increased concentration of adsorbate needs more active sites on adsorbent to shows the suitable adsorption capacity. According to the unchanged adsorbent concentration in the present evaluation, active sites are constant and the increasing of Zn ions could cause to decrease in removal percent.

The results and range analysis of Taguchi method experiments

The results of the Taguchi method experiment are shown in Table 3. From the results presented in Table 3, we can find out that for the combination of the five factors, the optimum is the condition combination in experiment fifteen, that is, pH 6.00, contact time 40 min, Temperature 50°C, adsorbent mass 0.4 g, and initial Zn (II) concentration 50 mg/L. Under this condition, the removal percent can reach 99.76%. For all of the experimental conditions, experiment 14 can reach the highest adsorption capacity of about 132.1663 mg/g. The results of range analysis are shown in Table 4. K1, K2, K3 and K4 are the average values of the results of each level in the Taguchi method experiment. Range values are the average values of K1, K2, K3 and K4. Based on the principle of "The larger the better," range analysis indicates the best levels for each single factor and shows which factor is the most important in the adsorption process. The results are concluded in Table 3.

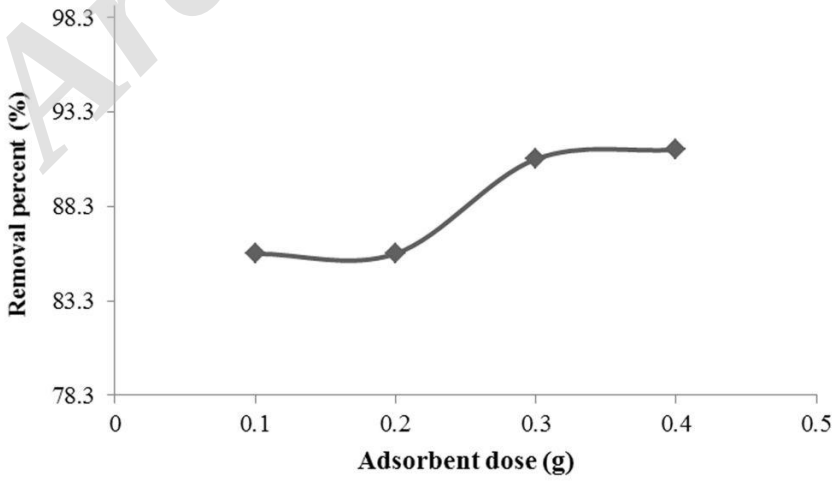

Fig. 7: The effect of adsorbent dose on the removal percent of Zn (II). Circles on figures indicate optimum dose for adsorption process.

Analysis of variance

The results of ANOVA for the Taguchi method experiment are given in Table 5. A statistical ANOVA was performed to see which process factors significantly affect the process responses. In the ANOVA, the Fischer ratio (or F test) was used to determine significant process factors. F test is a tool to see which process factor has a significant effect on removal percent.

According to the results and calculations, the influence of each parameter in the experiments' results is specified. In Zn (II) adsorption experiment of our pilot in the present paper, the influence of parameters is pH = 63.597%, temperature = 6.771 %, contact time = 0.000 %, adsorbent mass = 13.028% and initial Zn (II) = 8.253 %. Table 6 displays the optimum point obtained via the software. The optimum conditions include: pH = 6, Temperature = 35°C, adsorbent mass = 0.4 g, and initial Zn (II) = 50 mgL^{-1}. On the basis of the calculated F values, only pH inferred to have statistically significant influences on removal percent. Other factors show no significant effect on both adsorption capacity and

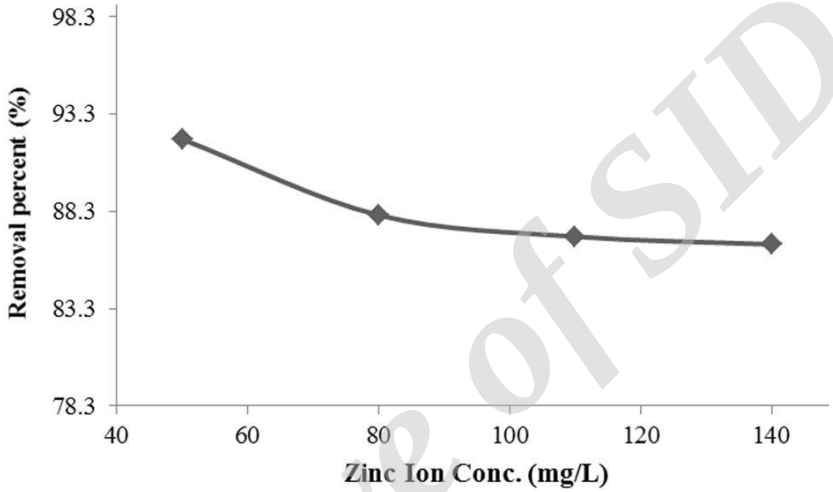

Fig. 8: The effect of initial concentration on the removal percent of Zn (II). Circles on figures indicate optimum concentration for adsorption.

Table 3: Design matrix and the experimental results for the L16 (45) orthogonal array experiment.

Experiment No.	Operating factors and their levels					Results	
	A	B	C	D	E	Adsorption capacity (mg/g)	Removal percent (%)
1	1	1	1	1	1	42.1663	84.33
2	1	2	2	2	2	32.0137	80.03
3	1	3	3	3	3	29.546	80.58
4	1	4	4	4	4	28	80
5	2	1	2	3	4	40.0033	85.72
6	2	2	1	4	3	25.1018	91.27
7	2	3	4	1	2	64.7075	80.88
8	2	4	3	2	1	21.1331	84.53
9	3	1	3	4	2	18.8603	94.301
10	3	2	4	3	1	16.59	99.54
11	3	3	1	2	4	60.3325	86.18
12	3	4	2	1	3	91.8888	83.53
13	4	1	4	2	3	50.9025	92.55
14	4	2	3	1	4	132.1663	94.4
15	4	3	2	4	1	12.47	99.76
16	4	4	1	3	2	25.925	97.21

The levels are shown in Table 1. Each value in the results is the mean of ten parallel ones A pH, B temperature, C contact time, D sorbent mass, E initial Zn (II) conc.

removal percent. The relative accuracy is 12.566 for removal percent. This is a very important finding since it indicates that the adsorption process was not influenced by the day and the environment, and it shows the stability and repeatability of the adsorption process.

Kinetics of adsorption

To study the kinetics of adsorption process two pseudo-first-order and pseudo-second-order models were evaluated. Equations 3 and 4 represent related equations respectively.

$$\ln [q_e - q_t] = \ln q_e - k_1 t \quad (3)$$

Table 4: Range analysis for the L_{16} (4^5) orthogonal array experiment.

	A	B	C	D	E
Removal percent					
K 1	81.235	89.225	89.747	85.784	92.04
K 2	85.599	91.309	87.26	85.822	88.105
K 3	90.887	86.849	88.452	90.762	86.982
K 4	95.98	86.317	88.242	91.332	86.574
Range	14.745	4.992	2.487	5.548	5.466

The levels are shown in Table 1, *A* pH, *B* temperature, *C* contact time, *D* sorbent mass, *E* initial Zn (II) conc. , K average value of each level, Range average value of K1, K2, K3and K4.

Table 5: ANOVA analysis for adsorption capacity and removal percent in the L_{16} (4^5) orthogonal array experimental design.

	Factor	DOF	Sum of squares (S)	Variance (V)	F-ratio (F)	Pure sum (S')	Percent P (%)
1	pH	3	491.279	163.759	39.094	478.713	63.597
2	Temperature	3	63.537	21.179	5.056	50.971	6.771
3	Time	(3)	(12.566)		POOLED		0.000
4	Absorbent	3	110.635	36.878	8.803	98.068	13.028
5	Concentration	3	74.689	24.896	5.943	62.123	8.253
	Other/Error	3	12.582	4.194			8.351
	Total	15	752.725				100.00%

A pH, *B* temperature, *C* contact time, *D* sorbent mass, *E* initial Zn (II)

Table 6: Optimum levels for each single factor in the L_{16}(4^5) orthogonal array experiment.

Factor	Level description	Level	Contribution
pH	6	4	7.554
Temperature	35°C	2	2.884
Absorbent	0.4g/100mL	4	2.907
Concentration	50 ppm	1	3.614
Total Contribution From All Factors	16.958		
Current Grand Average Of Performance	88.425		
Expected Result At Optimum Condition	105.384		

The levels are shown in Table 1, *A* pH, *B* temperature, *C* contact time, *D* sorbent mass, *E* initial Zn (II) conc.

$t/q_t = t/q_e + 1/k_2 q_e^2$ (4)

where, q_t and q_e are the mg of adsorbed solute per gram of the adsorbent at time t and at equilibrium respectively. k_1 and k_2 are the pseudo-first-order and pseudo-second-order rate constants respectively and *t* is time [3, 32].

Figs. 9 shows the curves related to the pseudo-first-order and pseudo-second-order models respectively. According to the results, the pseudo-second-order model well described the experimental data ($R^2 = 1$).

Adsorption isotherms

To evaluation the adsorption isotherms of removal of Zn ions by halloysite, Langmuir and Freundlich expressions were investigated. Equations 5 and 6 show Langmuir and Freundlich expressions.

$q_e = q_o k_l C_e/(1+k_l C_e)$ (5)

$q_e = k_f C_e^{1/n}$ (6)

where q_o and q_e are the maximum monolayer coverage capacity and the mg of adsorbed solute per gram of the adsorbent at equilibrium respectively. k_l and k_f are the Langmuir and Freundlich constants respectively. C_e is the equilibrium concentration of adsorbate (mg L^{-1}) and *n* is adsorption intensity [33].

As shown in Fig. 10 that corresponds to the Langmuir and Freundlich expressions, the Freundlich model fits well the experimental data indicating multilayer adsorption of the Zn ions at the outer surface of the HNTs particles. Therefore it seems that HNTs surface is heterogeneous and active sites and their energies distribute exponentially. First the stronger binding sites are occupied, and then by decreasing adsorption energy exponentially, the adsorption process is completed [34].

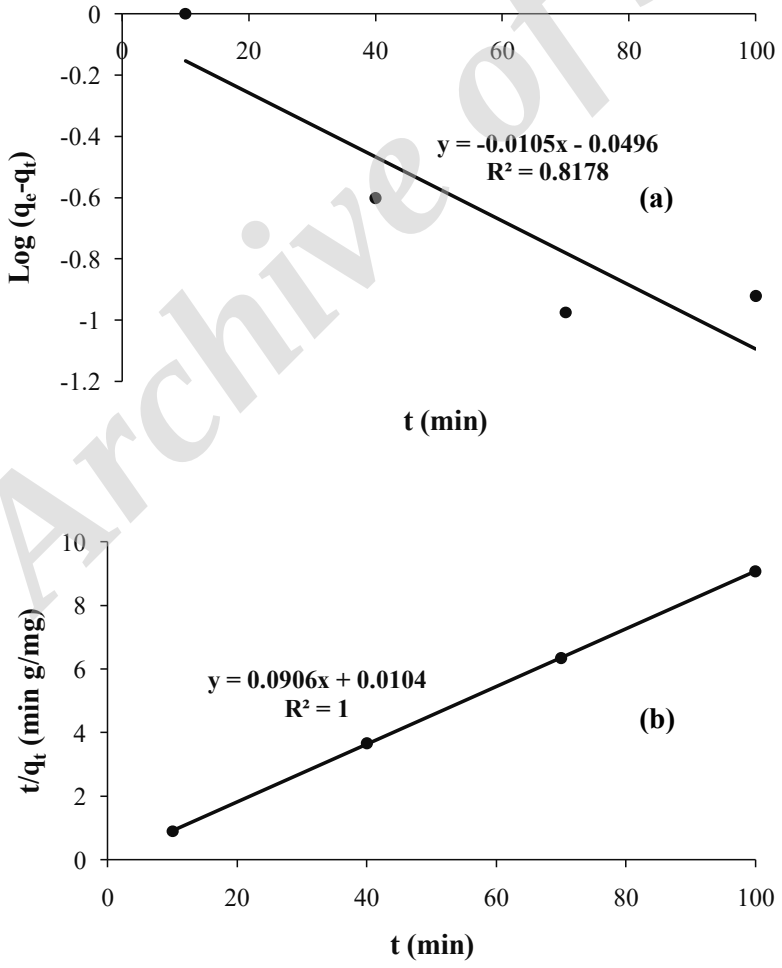

Fig. 9: Pseudo-first-order and pseudo-second-order plots for the adsorption of Zn ions onto HNTs.

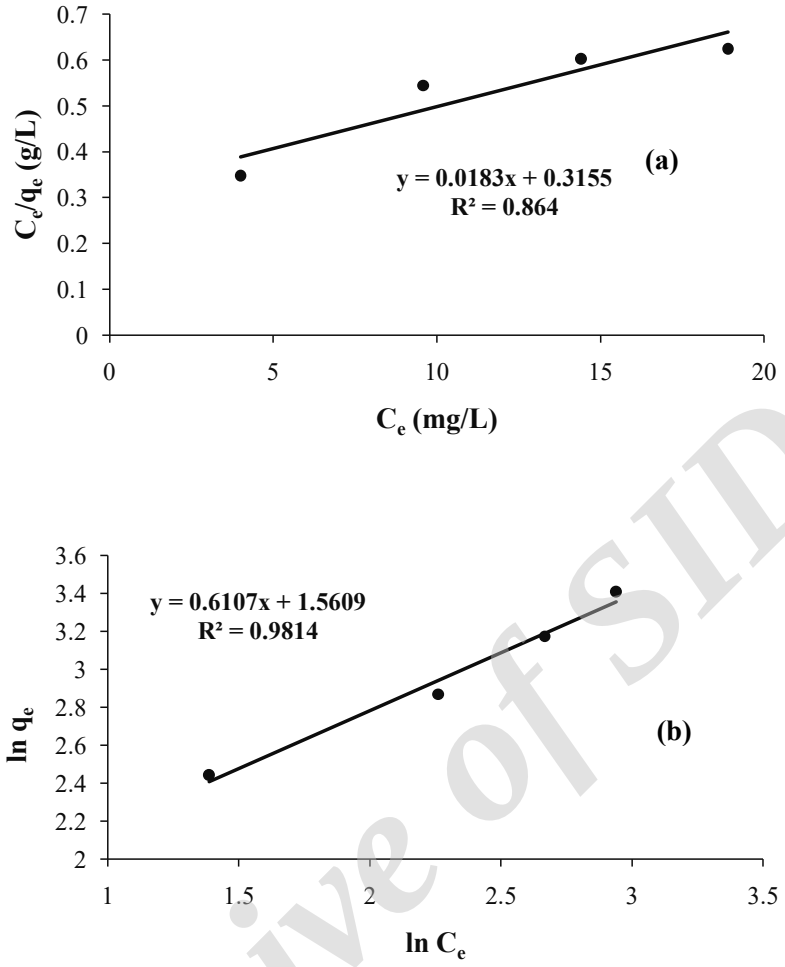

Fig. 10: Langmuir and Freundlich plots for the adsorption of Zn ions onto HNTs.

Adsorption thermodynamics

The amount of Zn ions adsorbed onto halloysite at equilibrium was used to calculation of thermodynamic parameter. Changes in the free energy (ΔG°) were calculated using equation 7.

$$\Delta G^\circ = -RT \ln K \quad (7)$$

where, R is the universal gas constant (8.314 J mol^{-1} K^{-1}), K is equilibrium constant, and T(K) is the temperature. The free energy changes (ΔG°) for Zn ions adsorbed onto halloysite in this work was calculated -3.997kJ mol^{-1} that indicates spontaneous physical sorption is dominant [3].

Comparison of Zn ions adsorption onto HNTs with other sorbents

Various adsorbents have been used to removal of Zn ions. The maximum adsorption capacity of different adsorbents were collected in Table 7 and compared with the present work [29, 35-44]. Although direct comparison of different adsorbents is difficult due to differences in experimental conditions, the adsorption capacity of HNTs in the present work is higher than that of magnetic chitosan cross-linked with glutaraldehyde, penicillium fellutinum (composite with bentonite), hydroxyapatite/chitosan composite, imine functionalized magnetic nanoparticles, g-MnO_2 nanostructures, sodium dodecyl sulphate coated magnetite nanoparticles, biogenic elemental selenium nanoparticles, magnetite silica core-shell nanoparticles, and HNTs reported in another paper and lower than that of magnetic chitosan modified with diethylenetriamine and succinyl-grafted chitosan. The excellent advantages of HNTs such as low cost, renewability, environmentally

Table 7: Comparison of Zn ions adsorption onto HNTs with other sorbents.

Sorbent	q_{max} (mg/g)	Reference
HNTs	9.9	29
Magnetic chitosan cross-linked with glutaraldehyde	32	37
Imine Functionalized Magnetic Nanoparticles	54.53	44
g-MnO_2 nanostructures	55.23	42
Sodium dodecyl sulphate coated magnetite nanoparticles	59.2	41
biogenic elemental selenium nanoparticles	60	43
Penicillium fellutinum (composite with bentonite)	78.5	39
Hydroxyapatite/chitosan composite	110	36
Magnetite Silica Core-Shell Nanoparticles	119	45
HNTs	132	This study
Magnetic chitosan modified with diethylenetriamine	180	38
succinyl-grafted chitosan	290	40

friendly feather, and naturally availability as well as supplying appropriate experimental condition make HNTs suitable and efficient adsorbent to removal of Zn ions [29].

CONCLUSIONS

In this study, HNTs was chosen as the adsorbent. The results confirm that it is more effective for the removal of Zn (II) compared with those found in the literatures without any chemical or physical pretreatment. From the Taguchi method, the optimum condition for removal percent was found out. Under these optimum conditions, adsorption capacity and removal percent obtained were 132.1663mg/g and 99.76%, respectively. Besides, range analysis and ANOVA results indicate that pH statistically inferred to have significance influences on removal percent. Other factors show no signs for removal percent. HNTs adsorbent is a relative low cost material that shows great potential to be applied in wastewater technology for remediation of toxic metals. Our findings may also have general industrial applications in the field of treatment and disposal of liquid hazardous waste.

ACKNOWLEDGEMENT

The authors thank the University of Tabriz, Iran for all the supports provided.

CONFLICT OF INTEREST

The authors declare that there is no conflict of interests regarding the publication of this manuscript.

REFERENCES

[1] Shah B. A., Shah A. V., Singh R. R., Patel N. B., (2011), Reduction of Cr (VI) in electroplating wastewater and investigation on the sorptive removal by WBAP. *Environ. Prog. Sustainable Energy*. 30: 59-69.

[2] Gerçel Ö., Gerçel H. F., (2007), Adsorption of lead (II) ions from aqueous solutions by activated carbon prepared from biomass plant material of Euphorbia rigida. *Chem. Eng. J.* 132: 289-297.

[3] Kiani G., Dostali M., Rostami A., Khataee A. R., (2011), Adsorption studies on the removal of Malachite Green from aqueous solutions onto halloysite nanotubes. *Applied Clay Sci.* 54: 34-39.

[4] Kiani G. R., Sheikhloie H., Arsalani N., (2011), Heavy metal ion removal from aqueous solutions by functionalized polyacrylonitrile. *Desalination*. 269: 266-270.

[5] Kiani G., Soltanzadeh M., (2014), High capacity removal of silver (I) and lead (II) ions by modified polyacrylonitrile from aqueous solutions. *Desal. and Water Treat*. 52: 3206-3218.

[6] Zargarlellahi H., Ghafourian H., (2014), Separation of heavy metal Nickel (II) using a new nano adsorbent string GZ-BAKI-TAC-Ni-88 from Ni contaminated Water using beshel tire activated Carbon. *Int. J. Nano Dimens.* 5: 197-202.

[7] Sadegh H., Ghoshekandi R. S., Masjedi A., Mahmoodi Z., Kazemi M., (2016), A review on Carbon nanotubes adsorbents for the removal of pollutants from aqueous solutions. *Int. J. Nano Dimens.* 7: 109-120.

[8] Kiani G., (2014), High removal capacity of silver ions from aqueous solution onto halloysite nanotubes. *Appl. Clay Sci.* 90: 159-164.

[9] Kiani G., (2015), Adsorption kinetics and thermodynamics of Malachite Green from aqueous solutions onto expanded

Graphite nanosheets. *Int. J. Nano Dimens.* 6: 55-66.
[10] Massaro M., Colletti C. G., Lazzara G., Guernelli S., Noto R., Riela S., (2017), Synthesis and characterization of Halloysite–Cyclodextrin nanosponges for enhanced dyes adsorption. *ACS Sustain. Chem. Eng.* 5: 3346-3352.
[11] Maziarz P., Prokop A., Matusik J., (2015), A comparative study on the removal of Pb (II), Zn (II), Cd (II) and As (V) by natural, acid activated and calcined halloysite. *Geology Geophys. Environ.* 41: 108-112.
[12] Ferrante F., Armata N., Cavallaro G., Lazzara G., (2017), Adsorption studies of molecules on the halloysite surfaces: A computational and experimental investigation. *J. Phys. Chem. C.* 121: 2951-2958.
[13] Deng L., Yuan P., Liu D., Annabi-Bergaya F., Zhou J., Chen F., Liu Z., (2017), Effects of microstructure of clay minerals, montmorillonite, kaolinite and halloysite, on their benzene adsorption behaviors. *Appl. Clay Sci.* 143: 184-191.
[14] Cataldo S., Lazzara G., Massaro M., Muratore N., Pettignano A., Riela S., (2018), Functionalized halloysite nanotubes for enhanced removal of lead (II) ions from aqueous solutions. *Appl. Clay Sci.* 156: 87-95.
[15] Massaro M., Campofelice A., Colletti C. G., Lazzara G., Noto R., Riela S., (2018), Functionalized halloysite nanotubes: Efficient carrier systems for antifungine drugs. *Appl. Clay Sci.* In press, corrected proof.
[16] Mishra S. P., Tiwari D., Dubey R. S., (1997), The uptake behaviour of rice (Jaya) husk in the removal of Zn (II) ions—A radiotracer study. *Appl. Radiat. Isotopes.* 48: 877-882.
[17] Chandra Srivastava V., Deo Mall I., Mani Mishra I., (2006), Modelling individual and competitive adsorption of cadmium (II) and zinc (II) metal ions from aqueous solution onto bagasse fly ash. *Separat. Sci. Technol.* 41: 2685-2710.
[18] Taguchi G., (1990), Introduction to Quality Engineering. McGraw-Hill, New York, USA.
[19] Chou C. S., Yang R. Y., Chen J. H., Chou S. W., (2010), The optimum conditions for preparing the lead-free piezoelectric ceramic of Bi 0.5 Na 0.5 TiO_3 using the Taguchi method. *Powder Technol.* 199: 264-271.
[20] Azghandi O. R., Maghrebi M. J., Teymourtash A. R., (2016) Modification of Glucose biosensor using Pt/MWCNTs electrode and optimization by application of taguchi method. *Int. J. Nano Dimens.* 7: 231-239.
[21] Ohdar N. K., Jena B. K., Sethi S. K., (2017), Optimization of EDM process parameters using Taguchi Method with Copper Electrode. *Int. Res. J. Eng. Technol.* 4: 2428-2431.
[22] Rahmani M., Kaykhaii M., Sasani M., (2018), Application of Taguchi L16 design method for comparative study of ability of 3A zeolite in removal of Rhodamine B and Malachite green from environmental water samples. *Spectrochim. Acta Part A: Molec. Biomolec. Spect.* 188: 164-169.
[23] Kıvak T., Mert Ş., (2017), Application of the Taguchi technique for the optimization of surface roughness and tool life during the milling of Hastelloy C22. *Mater. Testing*. 59: 69-76.
[24] Roy R. K., (2001), Design of experiments using the Taguchi approach: 16 steps to product and process improvement. *John Wiley & Sons.*
[25] Shah B. A., Shah A. V., Tailor R. V., (2011), Characterization of hydroxybenzoic acid chelating resins: Equilibrium, kinetics, and isotherm profiles for Cd (II) and Pb (II) uptake. *J. Serbian Chem. Soc.* 76: 903-922.
[26] Zou M., Du M., Zhu H., Xu C., Fu Y., (2012), Green synthesis of halloysite nanotubes supported Ag nanoparticles for photocatalytic decomposition of methylene blue. *J. Phys. D: Appl. Phys.* 45: 325302-325306.
[27] Gao Y., Fan C., Xu H., (2017), Experimental study on adsorption of rare earth elements on Kaolinite and Halloysite. *Acta Geologica Sinica (English Edition).* 91: 134-135.
[28] Kim K. J., Kreider P. B., Choi C., Chang C. H., Ahn H. G., (2013), Visible-light-sensitive Na-doped p-type flower-like ZnO photocatalysts synthesized via a continuous flow microreactor. *RSC Advances.* 3: 12702-12710.
[29] Dong Y., Liu Z., Chen L., (2012), Removal of Zn (II) from aqueous solution by natural halloysite nanotubes. *J. Radioanal. Nuclear Chem.* 292: 435-443.
[30] Saeed A., Iqbal M., Akhtar M. W., (2005), Removal and recovery of lead (II) from single and multimetal (Cd, Cu, Ni, Zn) solutions by crop milling waste (black gram husk). *J. Hazardous Mater.* 117: 65-73.
[31] Zolfaghari G., Esmaili-Sari A., Anbia M., Younesi H., Amirmahmoodi S., Ghafari-Nazari A., (2011), Taguchi optimization approach for Pb (II) and Hg (II) removal from aqueous solutions using modified mesoporous carbon. *J. Hazardous Mater.* 192: 1046-1055.
[32] Simonin J. P., (2016), On the comparison of pseudo-first order and pseudo-second order rate laws in the modeling of adsorption kinetics. *Chem. Eng. J.* 300: 254-263.
[33] Dada A. O., Olalekan A. P., Olatunya A. M., Dada O., (2012), Langmuir, Freundlich, Temkin and Dubinin–Radushkevich isotherms studies of equilibrium sorption of Zn^{2+} unto phosphoric acid modified rice husk. *IOSR J. Appl. Chem.* 3: 38-45.
[34] Saadi R., Saadi Z., Fazaeli R., Fard N. E., (2015), Monolayer and multilayer adsorption isotherm models for sorption from aqueous media. *Korean J. Chem. Eng.* 32: 787-799.
[35] Bazargan-Lari R., Bahrololoom M. E., Nemati A., (2011), Sorption behavior of Zn (II) ions by low cost and biological natural hydroxyapatite/chitosan composite from industrial waste water. *J. Food Agric. Environ.* 9: 892-897.
[36] Fan L., Luo C., Lv Z., Lu F., Qiu H., (2011), Preparation of magnetic modified chitosan and adsorption of Zn^{2+} from aqueous solutions. *Colloids and Surf. B: Biointerf.* 88: 574-581.
[37] Li H., Bi S., Liu L., Dong W., Wang X., (2011), Separation and accumulation of Cu (II), Zn (II) and Cr (VI) from aqueous solution by magnetic chitosan modified with diethylenetriamine. *Desalination*. 278: 397-404.
[38] Rashid A., Bhatti H. N., Iqbal M., Noreen S., (2016), Fungal biomass composite with bentonite efficiency for nickel and zinc adsorption: A mechanistic study. *Ecological Eng*. 91: 459-471.
[39] Kyzas G. Z., Siafaka P. I., Pavlidou E. G., Chrissafis K. J., Bikiaris D. N., (2015), Synthesis and adsorption application of succinyl-grafted chitosan for the simultaneous removal of zinc and cationic dye from binary hazardous mixtures. *Chem. Eng. J.* 259: 438-448.
[40] Adeli M., Yamini Y., Faraji M., (2017), Removal of copper, nickel and zinc by sodium dodecyl sulphate coated

magnetite nanoparticles from water and wastewater samples. *Arab. J. Chem.* 10: S514-S521.

[41] Dinh V. P., Le N. C., Nguyen N. T., Ho T. H., (2017), Comparison of the adsorption of Zn (II) on alpha-and gamma-MnO_2 nanostructures. *Vietnam J. Sci. Technol. Eng.* 59: 14-19.

[42] Jain R., Jordan N., Schild D., Van Hullebusch E. D., Weiss S., Franzen C., Lens P. N., (2015), Adsorption of zinc by biogenic elemental selenium nanoparticles. *Chem. Eng. J.* 260: 855-863.

[43] Ojemaye M. O., Okoh O. O., Okoh A. I., (2018), Uptake of Zn^{2+} and As^{3+} from wastewater by adsorption onto imine functionalized magnetic nanoparticles. *Water.* 10: 36-42.

[44] Emadi M., Shams E., Amini M. K., (2012), Removal of zinc from aqueous solutions by magnetite silica core-shell nanoparticles. *J. Chem.* 2013: 1-10.